

UDK 677.017.5; 625.074

Synthesis of Anatase Nanopowders by Sol-gel Method and Influence of Temperatures of Calcination to Their Photocatalytic Properties

A. Golubović^{1,*}, B. Simović², M. Šćepanović¹, D. Mijin³, A. Matković¹,
M. Grujić-Brojčin¹, B. Babić⁴

¹ Center for Solid State Physics and New Materials, Institute of Physics, University of Belgrade, Pregrevica 118, 11080 Belgrade-Zemun, Serbia

² Institute for Multidisciplinary Research, University of Belgrade, Kneza Višeslava 1, 11000 Belgrade, Serbia

³ Faculty of Technology and Metallurgy, University of Belgrade, Karnegijeva 4, 11120 Belgrade, Serbia

⁴ Institute of Nuclear Sciences "Vinča", University of Belgrade, 11001 Belgrade, Serbia

Abstract:

The titanium dioxide (TiO_2) nanopowders were produced by sol-gel technique from tetrabutyl titanate as a precursor, varying the temperature of calcination (from 500 to 550 °C with the step of 10 °C). XRPD results have shown that all synthesized nanopowders are dominantly in anatase phase. The analysis of the shift and linewidth of the most intensive anatase E_g Raman mode confirmed the XRPD results and added the presence of small amount of highly disordered brookite phase in all samples. The analysis of pore structure from nitrogen sorption experimental data described all samples as mesoporous, with mean pore diameters in the range of 1.5 and 4.5 nm. Nanopowder properties have been related to the photocatalytic activity, tested in degradation of the textile dye (C.I. Reactive Orange 16). The sample calcined at temperature of 510 °C showed the best photocatalytic performance.

Keywords: Nanopowders; Sol-gel; Porosity; Optical properties; TiO_2

1. Introduction

Permanent environmental pollution from industrial wastewater is of major concern. Many industries use dyes in order to colour their products and consume substantial volumes of water. Semiconductor photocatalysis is a very popular technology that has a lot of applications in environmental systems such as air purification, water disinfection, hazardous waste remediation, and water purification [1]. Several semiconductors have band gap energies sufficient for promoting or catalyzing a wide range of chemical reactions important for environmental. Among many candidates, TiO_2 has chosen to be the most suitable for widespread environmental applications because of its biological and chemical inertness, stability against photocorrosion and chemical corrosion, and cost-effectiveness [2]. Besides that, TiO_2 is the very important constituent of composite ceramic materials (binary, as Al_2O_3 - TiO_2 and TiO_2 - Y_2O_3 or ternary, as Al_2O_3 - TiO_2 - Y_2O_3) [3], and getting acquainted with

*) Corresponding author: golubovic@ipb.ac.rs

properties and abilities for applying can be necessary for possibility of composite applications.

The TiO₂/UV system has been widely investigated in heterogeneous photocatalysis [4]. UV irradiation upon a semiconductor can photoactivate TiO₂, generating electron/hole couples with strong redox properties for various environmental applications. However, the use of a TiO₂ photocatalyst in the photocatalytic oxidation of various pollutants is uncommon owing to its low photodegradation efficiency [5]. The photocatalytic efficiency of TiO₂ powder heavily depends on its microstructure and physical properties, which are in turn determined by the preparation conditions. Among these, the presence of mesopores gives rise to a large surface area, which offers abundant interaction sites with external molecules [6]. In this study, several methods of characterization, such as X-ray powder diffraction (XRPD), Brunauer-Emmett-Teller (BET) measurements, and Raman spectroscopy are employed in this study to investigate the influence of the TiO₂ nanopowders structure characteristics (the pore) caused by different synthesis conditions (the temperature of calcinations) to photocatalytic properties (photodegradation of the textile dye, C.I. Reactive Orange 16) of synthesized TiO₂ nanopowders.

2. Experimental details

2.1 Synthesis

The TiO₂ nanocrystals were prepared by a sol-gel method. The precursor in all experiments was tetrabutyl titanate (Ti(OBu)₄) and the molar ratio between reagents in the reaction of synthesis were Ti(OBu)₄:HCl:EtOH:H₂O = 1:0.3:15:4, where hydrochloride acid was used as the catalyst, ethanol as the solvent, and water for hydrolysis. The reaction of synthesis carried out at the temperature of ice, as the reaction polycondensation of Ti(OBu)₄ (aging). After the gelation, the wet gels were dried at 80°C, and then the dry gels were calcinated for 1.5 hours to obtain TiO₂ nanocrystals. The temperature of calcinations were 500 °C (T₅₀₀), 510 °C (T₅₁₀), 520 °C (T₅₂₀), 530 °C (T₅₃₀), 540 °C (T₅₄₀), and 550 °C (T₅₅₀), respectively. The heating rate and the cooling rate were the same, 135 °C/h, as in our previous experiments [7]. Ti(OBu)₄ was produced by Acros Organics, HCl by Zorka, Serbia, and C₂H₅OH by Carlo Erba. All chemicals were used without further purifications.

2.2 Characterization methods

X-ray powder diffraction (XRPD) patterns were obtained on an Ital Structures APD2000 X-ray diffractometer (Cu K α radiation, angular range: 20° < 2 θ < 70°). Data were collected at every 0.01° in the 10-70° 2 θ using a counting time of 80 s/step. The Fullprof computer program was used. The Williamson-Hall Method was applied for determination of the average microstrain and the mean crystallite sizes.

The powder was sonicated in ethanol for 15 minutes. Immediately afterwards, a drop of solution was casted onto a freshly cleaved kish graphite crystal embedded with a silver paste into a sample holder. Access material was removed in a stream of argon gas and the sample was left to degas in low vacuum for 1 hour, before the measurements on a scanning electron microscope (SEM). The measurements were carried out on a Tescan MIRA3 field emission gun SEM, at 10 kV in high vacuum. SEM working distance was about 4 mm. Sample plane was 40° tilted relative to the plane perpendicular to the SEM column axis.

Adsorption and desorption isotherms of N₂ were measured on TiO₂ samples, at -196°C, using the gravimetric McBain method. The specific surface area, S_{BET}, pore size distribution, mesopore including external surface area, S_{meso}, and micropore volume, V_{mic}, for the samples were calculated from the isotherms. Pore size distribution was estimated applying Barret-Joyner-Halenda (BJH) method [8] to the desorption branch of isotherms and mesopore

surface and micropore volume were estimated using the high resolution α_s plot method [9, 10]. Micropore surface, S_{mic} , was calculated by subtracting S_{meso} from S_{BET} .

Raman scattering measurements of TiO_2 samples were performed in the backscattering geometry at room temperature in the air using a TriVista T557 triple spectrometer with the 900/900/1800 grooves/mm gratings combination. The spectrometer was equipped with a confocal microscope and a nitrogen-cooled charge coupled device detector. The 514.5 nm line of a mixed Ar^+/Kr^+ gas laser was used as an excitation source with an output power of less than 5 mW to avoid local heating due to laser irradiation.

2.3 Measurements of photocatalytic activity

Procedure measurements of photocatalytic activity was the same as in [11], except the agitation in dark was 30 min instead 90 min. The textile dye, C.I. Reactive Orange 16, was obtained from Bezema as a gift (commercial name Bezaktiv Orange V-3R) and used without further purification.

3. Results and Discussion

3.1 Synthesis

In sol-gel synthesis experimental parameters were the same as in our previous experiments [7] except the duration of calcination of 4 hours. It was found that using the duration of 4 hours synthesized TiO_2 nanoparticles (anatase phase) have the best photocatalytic properties in photodegradation of metoprolol [12] within samples with various durations of calcinations (from 1 to 7 hours) and our samples have mentioned set-up of experimental parameters.

3.2 X-ray diffraction

Measured XPRD patterns for samples calcined at 500 °C and 550 °C are presented at Fig.1. Diffractograms of all samples were recorded, but there are very similar and only the most distant are presented. XRPD patterns of both samples (Fig. 1) are readily indexed to the anatase crystal structure (JCPDS card 21-1272, space group I41/amd). No impurities could be detected, meaning that single-phase TiO_2 powders were obtained. The crystal size of the TiO_2 nanopowders were calculated by Scherrer and Williamson-Hall methods and these values are presented in Tab. I.

Tab. I The unit cell parameters and unit cell volume, together with average crystallite size $\langle D \rangle$ of anatase and microstrain obtained by Scherrer and Williamson-Hall method.

Sample name	Unit cell parameters a, c [Å] V [Å ³]	Scherrer method $\langle D \rangle$ (nm)	Williamson-Hall method	
			$\langle D \rangle$ [nm]	Microstrain [%]
T_{500}	$a = 3.7820(2)$ $c = 9.509(7)$ $V = 136.01(1)$	22.6(4)	26.2(0)	0.08(4)
T_{550}	$a = 3.7806(2)$ $c = 9.5034(7)$ $V = 135.83(1)$	26.4(4)	32.3(1)	0.09(3)

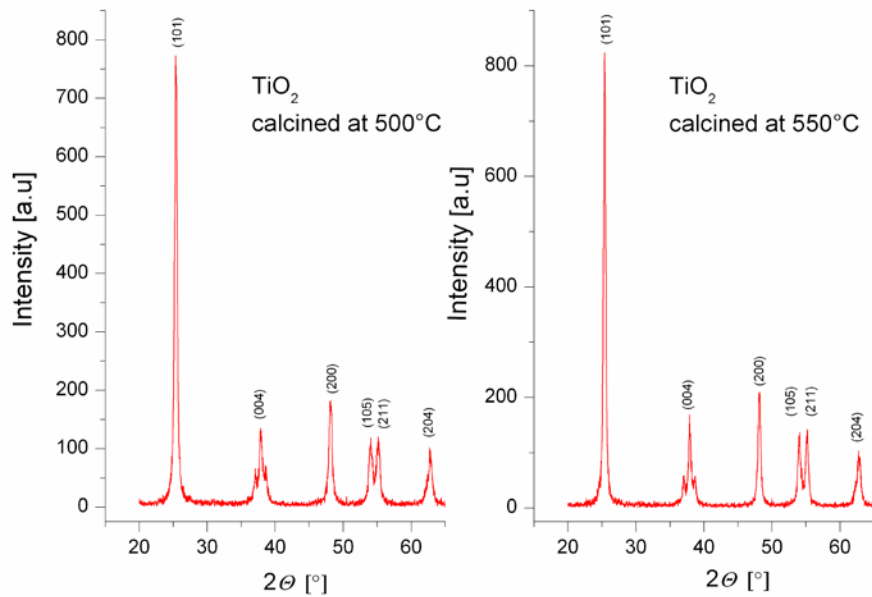


Fig. 1. XRD patterns of TiO_2 (T_{500} and T_{550}).

T_{500} sample has smaller crystallite size (Tab. I) compared to the T_{550} . The slight increasing of the crystallite size could be attributed to the change of temperature of calcination. Their positions are slightly shifted, indicating a change in lattice parameters in comparison to the bulk values for anatase which is accordance to values of crystallite sizes (nanopowders).

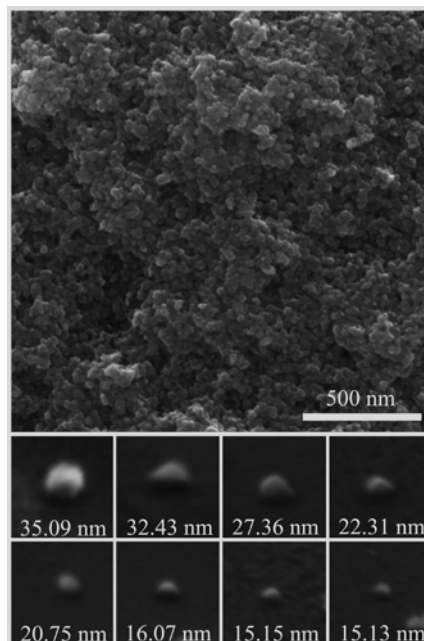


Fig. 2. Top: SEM image of the conglomerated structure for T_{500} formed out of single particles with an average radius of about 25 nm. The top image is magnified 400 \times . Bottom: eight single particles on graphite substrate. The size of each image is 100 nm \times 100 nm. The magnification of each bottom image is 1M \times . The diameter of each particle is estimated to be within ± 5 nm of the given value.

The results of SEM measurements for T_{500} are shown in Fig. 2. It could be clearly seen agglomerated structure which is accordance with the fact that pH value of gel equals point of zero charge (PZC) for TiO_2 obtained from tetrabutyl titanate [13] promotes higher agglomeration. Values of diameters of the individual particles in the sample T_{500} are in the range from 15-35 nm, whereas the average particle size is about 25 nm. The value of the average particle size is comparable with the crystallite size (26 nm) calculated by Williamson-Hall method.

Nitrogen adsorption isotherms for TiO_2 samples, as the amount of N_2 adsorbed as function of relative pressure at $-196\text{ }^\circ\text{C}$, are shown in Fig. 3. According to the IUPAC classification [14] isotherms of TiO_2 samples are of type IV and with a hysteresis loop which is associated with mesoporous materials. In all samples, the shape of hysteresis loop is of type H2 which indicates a poorly defined shape of pores [15]. Specific surface areas calculated by BET equation, S_{BET} , are listed in Tab. II. S_{BET} values, for all samples, lie within $16\text{-}32\text{ m}^2\text{ g}^{-1}$. Specific surface slightly decreases with increasing the temperature of calcination.

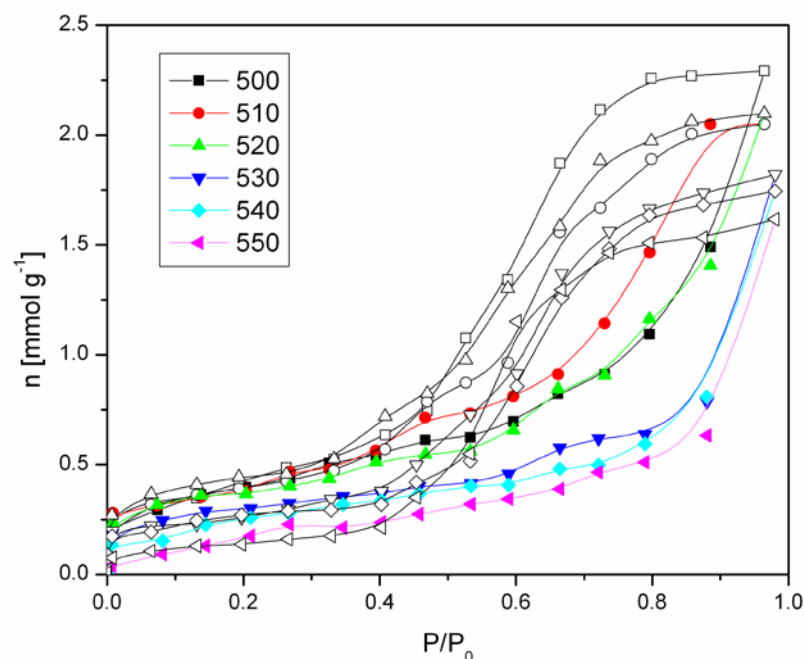


Fig. 3. Nitrogen adsorption isotherms, as the amount of N_2 adsorbed as function of relative pressure for TiO_2 samples. Solid symbols - adsorption, open symbols – desorption.

Tab. II Porous properties of TiO_2 samples (S_{BET} , S_{BJH}).

Sample	$S_{BET}=S_{meso}$ [m^2/g]
T_{500}	32
T_{510}	29
T_{520}	28
T_{530}	24
T_{540}	21
T_{550}	16

Pore size distribution (PSD) of TiO_2 samples is shown in Fig. 4. Figure shows that samples are mesoporous, with bimodal PSD for samples 500-530. PSD for 540 and 550 samples has a single peak. The most of the pores radius lies between 1.5 and 4.5 nm.

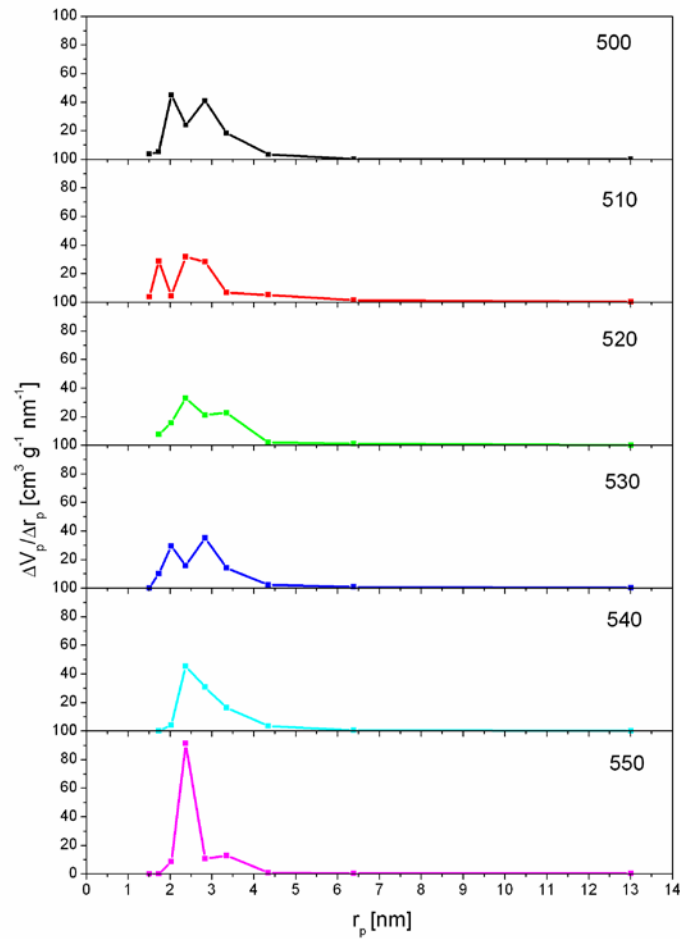


Fig. 4. Pore size distribution (PSD) for TiO₂ samples.

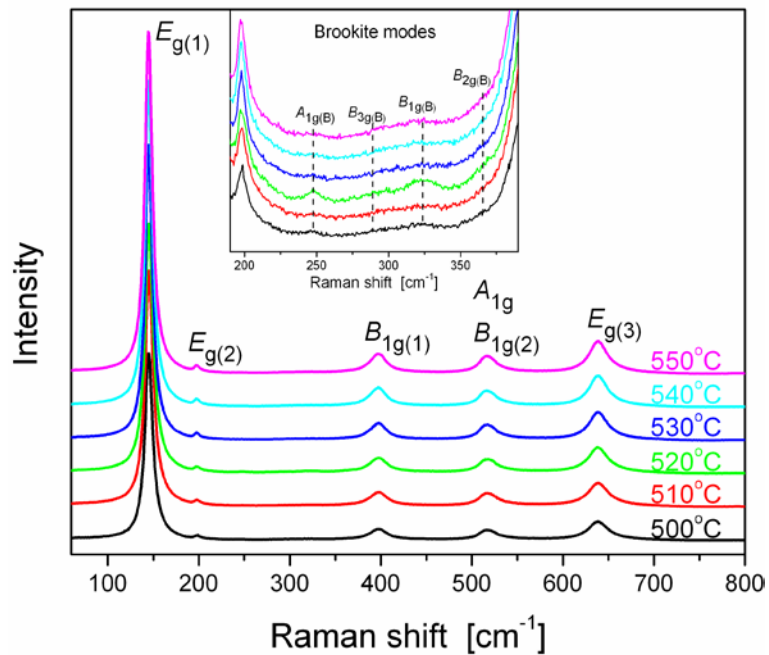


Fig. 5. Raman spectra of TiO₂ samples calcined at different temperatures with anatase modes denoted. Inset: the spectral region of 220–380 cm⁻¹ with characteristic brookite modes.

The Raman spectra presented in Fig. 5 have shown that dominant phase in all investigated TiO₂ samples was anatase as the most prominent Raman features have been assigned to this phase [16]: E_{g(1)} (~145 cm⁻¹), E_{g(2)} (~199 cm⁻¹), B_{1g}(~399 cm⁻¹), A_{1g} and B_{1g} (~518 cm⁻¹), and E_{g(3)} (~639 cm⁻¹). The intensity of anatase modes increased when calcination temperature increased. Also, blue shift and broadening of the most intensive anatase E_{g(1)} mode were little bit smaller for the samples calcined at higher temperatures. Both of these experimental findings confirmed well known fact that anatase nanocrystals were growing in size with the increase of calcination temperature [7]. Besides anatase modes, some additional features of very low intensity in the range from 220 to 380 cm⁻¹ (inset of Fig. 5) can be ascribed to the Raman modes of brookite phase [17]: A_{1g} (~247 cm⁻¹), B_{3g} (~287 cm⁻¹), B_{1g} (~322 cm⁻¹), and B_{2g} (~366 cm⁻¹). Low intensities and large line width softening modes should indicate that brookite phase was highly disordered [7, 17]. This fact is the reason while is the brookite phase invisible in XRPD analysis.

The photocatalytic activity of synthesized catalyst was studied using C.I. Reactive Orange 16 (textile dye) and results are presented in Fig. 6. The time after the agitation 30 min in dark is denoted as 0, and these concentrations are denoted as C₀. The results are shown in

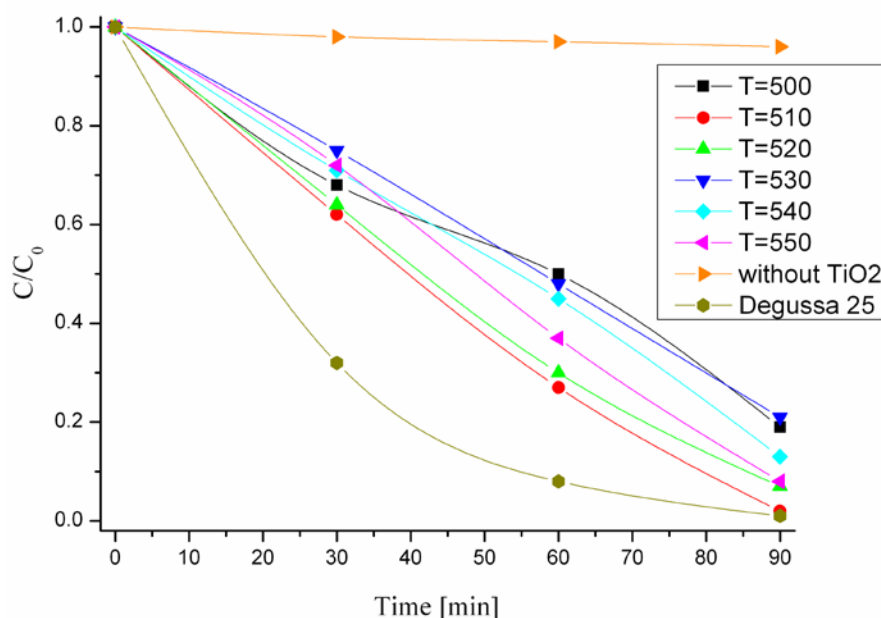


Fig. 6. The kinetics of photodegradation of C.I. Reactive Orange 16 under UV irradiation monitored in the presence of synthesized TiO₂ samples.

The photocatalytic process involves the separation of the electron-hole charge pair, their transport and trapping to/at the surface, and, finally, their reaction with the desired molecules. These processes always compete with the charge pair recombination. The nanostructure significantly affects these elemental processes based on several reasons. Apart from a high surface-to-volume ratio, which must be beneficial for all chemical processes, the first factor is, the quantum confinement and improved reduction/oxidation power. The second factor is the practical absence of band bending and the consequent easier access of both charged particles to the surface [18]. In our process of photocatalysis, the best results were obtained with catalyst T₅₁₀, with decolourisation effectiveness comparable with Degussa P25, almost 100 % after 90 min. There is no linear correlation between specific surface area of samples calculated by BET method and their photocatalytic degradation. Specific surface area of sample decreased with increasing temperature of the calcinations, while the behaviour of the photodegradation did not follow this rule. Taking Figs. 4 and 6 in account for a discussion about photocatalytic properties of TiO₂ series, maybe better explanation is the shape of the

distribution of pores (Fig. 4). All samples showed mesoporous structure, while the distribution and sizes were different. Applying Figs. 4 and 6, it could be notify tendency that samples T₅₁₀ and T₅₂₀ have a similar shape of pores distribution and the highest photocatalytic activity. The couple T₅₄₀-T₅₅₀ had a similar shape of pores distribution and their photocatalytic activity were also the similar. At the end, the couple T₅₀₀-T₅₃₀ had a similar shape of pores distribution and their photocatalytic activity were the similar and the worst in comparison to the other samples.

4. Conclusions

Mesoporous anatase nanopowders were synthesized by sol-gel method using tetrabutyl titanate as precursor. The structural and morphological properties of these powders were intentionally varied by temperature with the same duration of the calcination. The analysis of XRPD data showed that rising crystallite sizes (from 26.2 to 32.35 nm, estimated by Williamson-Hall method) with the rising temperatures of calcinations, and these results are in accordance to SEM data. Raman scattering data confirmed the anatase as dominant TiO₂ phase with a small amount of highly disordered brookite phase. The BET analysis showed that specific surface area was decreased in the samples when the temperature of calcination was increased. The sample calcined at 510 °C was displayed higher photocatalytic performances in the degradation and it was showed almost the same properties as commercial Degussa P25.

Acknowledgment

This work was financially supported by the Serbian Ministry of Education and Science Projects No. III45018 and OI171032 as well as SASA project F-134.

5. References

1. J. Fenoll, P. Sabater, G. Navarro, N. Vela, G. Pérez-Lucas, S. Navarro, J. Environ. Manage., 130 (2013) 361-368.
2. F. Gottschalk, T. Sun, B. Nowack, Environ. Pollut., 181 (2013) 287-300.
3. M. Vlasova, M. Kakazey, P. A. Márquez Aguilar, E.A. Juárez-Arellano, R. Guardian Tapia, V. Stetsenko, A. Bykov, S. Lakiza, A. Ragulya, Sci. Sinter. 45 92013) 247-259
4. S. S. Shinde, C. H. Brosale, K. Y. Rajpure, Catal. Rev., 55 (2013) 79-133.
5. K. Hashimoto, H. Irie, A. Fujishima, Jpn. J. Appl. Phys., 44 (2013) 8269-8285.
6. W. Li, X. Guo, Y. Zhu, Y. Hui, K. Kanamori, K. Nakanishi, J. Sol-Gel Sci. Technol., 67: (2013) 639-645.
7. A. Golubović, M. Šćepanović, A. Kremenović, S. Aškračić, V. Berec, Z. Dohčević-Mitrović, Z. V. Popović, J Sol-Gel Sci Technol., 49 (2009) 311-319.
8. E. P. Barret, L. G. Joyner, P. P. Halenda, J. Am. Chem. Soc., 73 (1951) 373-380.
9. K. Kruk, M. Jaroniec, K. P. Gadakaree, J. Colloid Interface Sci., 192 (1997) 250-256.
10. K. Kaneko, C. Ishii, H. Kanoh, Y. Hanzawa, N. Setoyama, T. Suzuki, Adv. Colloid Interface Sci., 76-77 (1998) 295-320.
11. A. Golubović, I. Veljković, M. Šćepanović, M. Grujić-Brojčin, N. Tomić, D. Mijin, B. Babić, J. Serb. Chem. Soc., (accepted for the publication)

12. A. Golubović, B. Abramović, M. Šćepanović, M. Grujić-Brojčin, S. Armaković, I. Veljković, B. Babić, Z. Dohčević-Mitrović, Z. V. Popović, Mater. Res. Bull., 48 (2013) 1363-1371.
13. M. Koslulski, Chemical Properties of Material Surface, Marcel Dekker, New York, USA, 2001, p. 42
14. K. S. W. Sing, D. H. Everett, R. A. W. Haul, L. Moscou, R. A. Pierotti, J. Rouquerol, T. Siemieniewska, Pure Appl. Chem., 57 (1985) 603-619.
15. S. Lowell, J.E. Shields, M. A. Thomas, M. Thommes, Characterization of Porous Solids and Powders: Surface Area, Pore Size and Density, Ed. Kluwer Academic Publishers, Dordrecht Netherlands, 2004, p. 44.
16. T. Ohsaka, F. Izumi, Y. Fujiki, J. Raman Spectrosc., 7 (1978) 321-324.
17. G. A. Tompsett, G. A. Bowmaker, R. P. Cooney, J. B. Metson, K. A. Rodgers, J. M. Seakins, J. Raman Spectrosc. 26 (1995) 57-62.
18. M. Fernández-García, A. Martínez-Arias, J. C. Hanson, J. A. Rodriguez, Chem. Rev. 104 (2004) 4063-4104.

Садржај: Прахови титанијум диоксида (TiO_2) су добијени сол-гел техником полазећи од тетрабутил-титаната уз варирање температура калцинације (од 500 to 550 °C са кораком од 10 °C). XRPD резултати су показали да синтетисани нанопрахови поседују анатас фазу. Анализа помераја и полуширине најинтезивнијег раманског мода E_g је потврдила XRPD резултате и утврдила код свих узорака постојање мале количине високо дезоријентисане фазе брукита. Анализа структуре пора из експерименталних података сорпције азота је показала постојање мезопора чије се средње величине крећу у опсегу од 1.5 до 4.5 nm. Фотокаталитичке особине нанопрахова су тестиране деградацијом текстилне боје (C.I. Reactive Orange 16). Узорак калцинисан на 510 °C је показао најбоља фотокаталитичка својства.

Кључне речи: нанопрахови; сол-гел; порозност; оптичке особине; TiO_2
